This article was downloaded by:
On: *15 January 2011*
Access details: *Access Details: Free Access*
Publisher *Taylor & Francis*
Informa Ltd Registered in England and Wales Registered Number: 1072954 Registered office: Mortimer House, 37-41 Mortimer Street, London W1T 3JH, UK

Comments on Inorganic Chemistry
Publication details, including instructions for authors and subscription information:
http://www.informaworld.com/smpp/title~content=t713455155

Intersystem Crossing in Iron(II) Coordination Compounds: A Model Process Between Classical and Quantum Mechanical Behaviour

Andreas Hauser[a]
[a] Institut für Anorganische und Physikalische Chemie, Universität Bern, Bern 9, Switzerland

To cite this Article Hauser, Andreas(1995) 'Intersystem Crossing in Iron(II) Coordination Compounds: A Model Process Between Classical and Quantum Mechanical Behaviour', Comments on Inorganic Chemistry, 17: 1, 17 — 40
To link to this Article: DOI: 10.1080/02603599508035780
URL: http://dx.doi.org/10.1080/02603599508035780

PLEASE SCROLL DOWN FOR ARTICLE

Full terms and conditions of use: http://www.informaworld.com/terms-and-conditions-of-access.pdf

This article may be used for research, teaching and private study purposes. Any substantial or systematic reproduction, re-distribution, re-selling, loan or sub-licensing, systematic supply or distribution in any form to anyone is expressly forbidden.

The publisher does not give any warranty express or implied or make any representation that the contents will be complete or accurate or up to date. The accuracy of any instructions, formulae and drug doses should be independently verified with primary sources. The publisher shall not be liable for any loss, actions, claims, proceedings, demand or costs or damages whatsoever or howsoever caused arising directly or indirectly in connection with or arising out of the use of this material.

Intersystem Crossing in Iron(II) Coordination Compounds: A Model Process Between Classical and Quantum Mechanical Behaviour

ANDREAS HAUSER
Institut für Anorganische und Physikalische Chemie,
Universität Bern,
Freiestrasse 3,
CH-3000 Bern 9, Switzerland

Received August 16, 1994

Downloaded At: 12:45 15 January 2011

Intersystem crossing is the crucial first step determining the quantum efficiency of very many photochemical and photophysical processes. Spin-crossover compounds of first-row transition metal ions, in particular of Fe(II), provide model systems for studying it in detail. Because in these compounds there are no competing relaxation processes, intersystem crossing rate constants can be determined over a large temperature interval. The characteristic features are tunnelling at temperatures below ~80 K and a thermally activated process above ~100 K. This, as well as the twelve order of magnitude increase of the low-temperature tunnelling rate constant on going from a spin-crossover compound with a small zero-point energy difference to a low-spin compound with a substantially larger one, can be understood on the basis of a nonadiabatic multiphonon process in the strong vibronic coupling limit.

Key Words: *intersystem crossing, spin-crossover, iron(II) coordination compounds, nonadiabatic multiphonon relaxation, strong vibronic coupling limit, tunnelling*

1. INTRODUCTION

Intersystem crossing (ISC), that is, the radiationless transition between electronic states of a system involving a change in spin

Comments Inorg. Chem.
1995, Vol. 17, No. 1, pp. 17–40
Reprints available directly from the publisher
Photocopying permitted by license only

© 1995 OPA (Overseas Publishers Association)
Amsterdam B.V.
Published under license by
Gordon and Breach Science Publishers S.A.
Printed in Malaysia

quantum number S, is one of the most simple yet universal radiationless processes in chemistry and physics. In very many photochemical and photophysical processes of technological relevance it constitutes the crucial first step, taking the system from the initially excited and usually short-lived state to the metastable state with a lifetime long enough for the processes of interest to actually have a chance of occurring. The three-level ruby laser,[1] for example, is based on the ISC step from the initially excited $^4T_2$ to the metastable ^2E state and the subsequent radiative transition back to the $^4A_2$ ground state of Cr(III) doped into Al_2O_3. In a more recent application, the ISC process from an excited ^{1}MLCT to the low-lying ^{3}MLCT state of $[Ru(bpy)_3]^{2+}$ (bpy = 2,2′-bipyridin) led to the development of a photovoltaic cell, making use of the resulting photoredox properties.[2]

For a given photochemical or photophysical process to be of potential technological use, its quantum efficiency must be above some limiting value. Thus the success of the above examples is due to quantum efficiencies of the respective ISC processes of close to one. However, this is the case for but a few Cr(III) as well as Ru(II) complexes. Particularly for the former, there is a vast and controversial literature discussing the reasons for the observed variation in photophysical and photochemical behaviour.[3]

Given the central role of ISC processes in photochemistry and photophysics, it is of paramount importance to arrive at a clear understanding of the parameters which govern their rates and their quantum efficiencies. The theoretical background to this problem was provided quite some time ago in the shape of the theory of nonadiabatic multiphonon relaxation.[4,5] This theory has been successfully applied to radiationless transitions in complexes of rare earth ions, that is, in the weak vibronic coupling limit, with small horizontal and comparatively large vertical displacements of the potential wells of the f states relative to each other.[6] For transition metal ions the situation is different: due to the larger effect of the ligands on the d orbitals, they show a much larger diversity in their electronic structure and bonding properties. As a consequence there is a large variation in the horizontal displacements of the relevant states relative to each other. Since in general excited state geometries are only accessible indirectly from spectroscopic data,[7] the all important reaction coordinate for ISC processes, and indeed for most other processes, is not usually known at the required level of accuracy. Thus, more often than

Downloaded At: 12:45 15 January 2011

not, estimates of ISC rate constants for transition metal complexes are off by many orders of magnitude.

Spin-crossover compounds of first-row transition metal ions provide the ideal systems to study the dynamics of ISC processes. Buhks *et al.*[8] suggested at quite an early stage that in these compounds the high-spin → low-spin relaxation should be regarded as a nonadiabatic multiphonon process in the strong vibronic coupling limit. Despite this, it continued to be treated mostly in terms of classical transition state theory.[9,10] This is in all probability due to the fact that the majority of studies have been performed in solution at ambient temperatures, and that Arrhenius plots of the observed rate constants usually gave straight lines over the limited temperature range accessible. However, for Fe(II) compounds it has been shown that at temperatures below ~100 K there are strong deviations from such a classical behaviour towards temperature independent tunnelling.[11,12]

Classical and semi-classical theories, i.e., transition state theory and Marcus' Theory, have been compared to multiphonon relaxation before,[13] and the limits of their respective validity have been thoroughly expounded. The aim of this *Comment* is to discuss a real process, namely the high-spin → low-spin relaxation in spin-crossover compounds, as a model process between classical and quantum mechanical behaviour.

For all those who are not familiar with the phenomena, Section 2 contains the briefest of introductions on thermal and light-induced spin transitions. Section 3.1 gives a review of the experimental results on relaxation dynamics both in the solid state and in solution, followed by theoretical considerations and a discussion in Sections 3.2 and 3.3, respectively. In the final section, conclusions regarding ISC processes in other systems are attempted.

2. THERMAL AND LIGHT-INDUCED SPIN TRANSITIONS

Octahedral complexes of transition metal ions with a d^4 to d^7 electron configuration can either have a low-spin (LS) ground state, with as many electrons as possible paired up in the t_{2g} orbitals, or a high-spin (HS) ground state with the electrons occupying the d orbitals according to Hund's Rule. The former situation is the result of a strong ligand field, the latter of a weak one. If for a given ligand

Downloaded At: 12:45 15 January 2011

the zero-point energy difference between the HS and the LS state $\Delta E^0_{HL} = E^0_{HS} - E^0_{LS}$ is positive and of the order of k_BT, a thermal transition from the LS state at low temperatures to an almost quantitative, entropy-driven population of the HS state at elevated temperatures may be observed.[14] Figure 1 shows the potential wells of the $^1A_1$ (LS) and the $^5T_2$ (HS) state appropriate for an Fe(II) spin-crossover compound with six d-electrons. The transition temperature $T_{1/2}$, defined as the temperature at which the HS fraction γ_{HS} is equal to the LS fraction γ_{LS}, is a measure for ΔE^0_{HL}, but the exact relationship between the two is not known *a priori*. For dilute systems $T_{1/2} = \Delta H^0_{HL}/\Delta S^0_{HL}$, but as both ΔH^0_{HL} and ΔS^0_{HL} are temperature dependent,[15] it is not possible to just set ΔE^0_{HL} equal to ΔH^0_{HL}! However, ΔE^0_{HL} can be set equal to ΔG^0_{HL} ($T \rightarrow 0$), which can be extrapolated from experimental thermal transition curves. In Table I values for ΔE^0_{HL} and $T_{1/2}$ for the much investigated complex $[Fe(pic)_3]^{2+}$ in a number of dilute mixed crystal matrices as well as in aqueous solution taken from Refs. 16 and 17 are given. The different matrices exert varying internal or chemical pressures and thus influence ΔE^0_{HL}. Figure 2 shows ΔE^0_{HL} as a function of $T_{1/2}$ for the $[Fe(pic)_3]^{2+}$ series. Within limits, this curve may be considered typical for Fe(II) coordination compounds.

The simplistic treatment of the spin transition as a unimolecular process exhibiting a temperature dependent LS $\rightleftarrows$ HS equilibrium is valid for spin-crossover complexes in solution, in amorphous matrices and in dilute mixed crystal systems. In concentrated crystalline materials, cooperative effects have to be taken into account. Those will not be discussed in this *Comment*.

In addition to the two low-energy ligand field states responsible for the thermal spin transition, spin-crossover compounds possess excited ligand field as well as charge transfer states (see Fig. 1). Some ten years ago Decurtins *et al.*[18] discovered that in Fe(II) systems in the solid state it is possible to achieve complete light-induced LS $\rightarrow$ HS conversions well below the thermal transition temperatures by irradiating either into spin-allowed d-d or MLCT bands. At 20 K lifetimes of these metastable HS states of up to 10^6 s were observed. A mechanism for the light-induced spin transition was proposed[18] and justified experimentally.[19] It involves several extremely rapid ISC steps ($k > 10^{12}$ s^{-1} [20]) between excited states, the energy barrier due to the large change in metal–ligand bond length Δr_{HL} of ~0.16–

Downloaded At: 12:45 15 January 2011

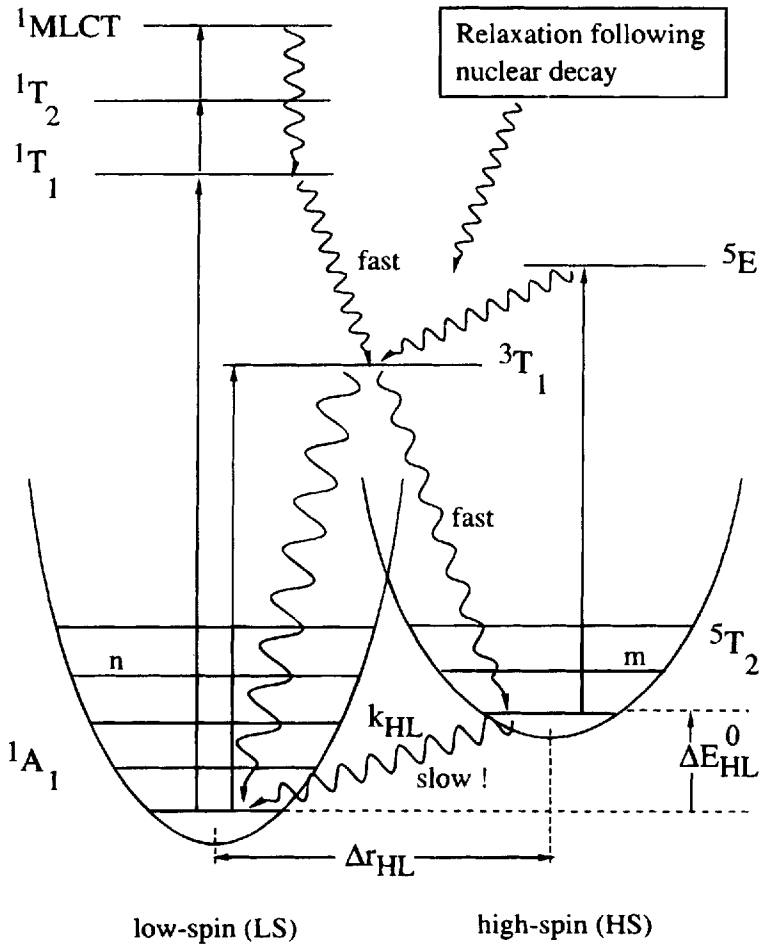

FIGURE 1 Configurational coordinate diagram appropriate for a d^6 spin-crossover system. Arrows indicate the mechanism of light-induced processes.

Downloaded At: 12:45 15 January 2011

TABLE I

Transition temperatures $T_{1/2}$ and zero-point energy differences $\Delta E^0_{HL} = \Delta G^0_{HL}(T \rightarrow 0)$ for the $[Fe(pic)_3]^{2+}$ spin-crossover complex in a number of crystalline host materials in low concentrations.

Host	$T_{1/2}$ [K]	ΔE^0_{HL} [cm^{-1}]
$[Mn(NH_2\text{-}pic)_3]Cl_2 \cdot EtOH$	75	80
$[Zn(NH_2\text{-}pic)_3]Cl_2 \cdot EtOH$	78	95
$[Co(NH_2\text{-}pic)_3]Cl_2 \cdot EtOH$	89	115
$[Zn(ND_2\text{-}pic)_3]Cl_2 \cdot EtOH$	102	181
$[Mn(NH_2\text{-}pic)_3]Cl_2 \cdot MeOH$	117	204
$[Zn(NH_2\text{-}pic)_3]Cl_2 \cdot MeOH$	140	320
$[Co(NH_2\text{-}pic)_3]Cl_2 \cdot MeOH$	148	338
$[Zn(ND_2\text{-}pic)_3]Cl_2 \cdot MeOH$	154	377
$[Fe(pic)_3]^{2+}$ in H_2O	295	900

All values from Refs. 16 and 17.

Downloaded At: 12:45 15 January 2011

0.21 Å[10,21,22] being responsible for the trapping of the HS state at lov enough temperatures. First observations of such long-lived metasta ble HS states were made for neat spin-crossover compounds, bu later they were found both for spin-crossover complexes in dilut mixed crystals[23] as well as embedded in polymer matrices.[24] Thu the long lifetime of the trapped HS state is really a property of th individual complex.

Transient populations of the HS state are also possible at elevatec temperatures. In fact, prior to the discovery of Decurtins *et al.* McGarvey and Lawthers[25] noticed a rapid depopulation of the ^1A state in some Fe(II) compounds upon pulsed laser irradiation, bu with relaxation rates on the order of 10^7 s^{-1} in solution and a ambient temperatures, their light-induced states were comparatively short-lived.

In addition, transient populations of the $^5T_2$ state have been found for Fe(II) low-spin complexes such as $[Fe(bipy)_3]^{2+}$ following pulsed laser excitation both at room temperature in solution[26] as well as at cryogenic temperatures in the solid state,[27] and as an after-effect of the nuclear decay of ^{57}Co.[28] The Mössbauer emission study of Deisenroth *et al.*, in fact, proves the transient state to be the $^5T_2$ state.

No long-lived HS states have been observed at low temperatures for Fe(III) and Co(II) spin-crossover systems so far. Indeed, none

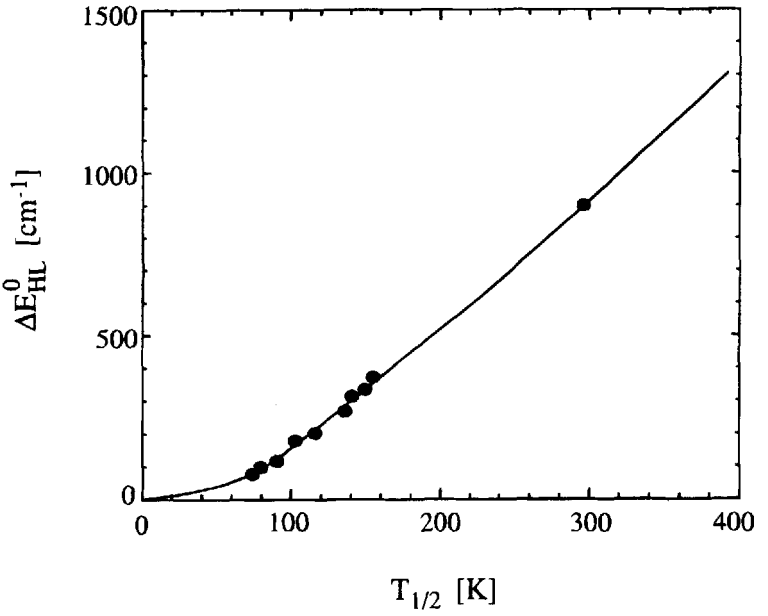

FIGURE 2 The zero-point energy difference ΔE^0_{HL} as a function of the transition temperature of the thermal spin transition $T_{1/2}$ for the spin-crossover complex $[Fe(pic)_3]^{2+}$ in various matrices (according to Table I).

Downloaded At: 12:45 15 January 2011

are expected (*vide infra*), but Lawthers and McGarvey[29] once again observed a light-induced perturbation of the $^2T_2 \leftrightarrow {}^6A_1$ equilibrium in some Fe(III) systems in solution.

3. THE LS ⇄ HS RELAXATION DYNAMICS

3.1 Experimental Results

Initial studies on the LS ⇄ HS relaxation dynamics in spin-crossover compounds were mostly performed at ambient temperatures in solution,[9] using such diverse methods as Raman temperature jump techniques,[30] ultrasonic relaxation,[31] and laser perturbation.[25,32] In solution only a limited temperature range is accessible and (except for laser perturbation) studies are restricted to systems with transition tempera-

tures $T_{1/2}$ within this range, because these methods require both species of the unimolecular process to be present in a dynamic equilibrium. The relaxation rate constants for the forward and back reaction can be calculated from the observed relaxation rate constant:

$$k_{obs} = k_{LH} + k_{HL} = k_{HL}(1 + K), \tag{1}$$

where the equilibrium constant K is given by

$$K = \frac{\gamma_{HS}}{\gamma_{LS}} = \frac{k_{LH}}{k_{HL}} = \exp(-\Delta G^0_{HL}/k_B T). \tag{2}$$

Arrhenius or Eyring plots of the experimentally determined rate constants according to Eqs. (3) and (4), respectively:

$$k = A \exp(-E^a/k_B T), \tag{3}$$

$$k = \frac{k_B T}{h} \exp(-(\Delta H^* - T\Delta S^*)/k_B T), \tag{4}$$

usually gave straight lines, from which activation parameters were extracted. Table IIa gives k_{HL} at 295 K, activation energies E^a_{HL}, frequency factors A_{HL}, as well as transition temperatures $T_{1/2}$ calculated from the activation parameters collected by Refs. 9 and 10 for a series of Fe(II) spin-crossover compounds in solution. There is no obvious correlation between any of these quantities! In addition, Table IIa includes the results of laser perturbation experiments on three low-spin compounds.[10,20,33] The only thing to note at this stage is the comparatively small range of 10^6–10^8 s^{-1} spanned by k_{HL} at room temperature for the spin-crossover systems and the somewhat higher values for the low-spin systems.

Similar LS $\rightleftarrows$ HS relaxation rate constants and activation parameters as in solution were obtained for some Fe(II) spin-crossover systems at ambient temperatures in the solid state using line-shape analysis of Mössbauer spectra.[34] Unfortunately this technique is restricted to the small range of rate constants $\sim 10^6$–10^8 s^{-1} and requires both species to be present in appreciable amounts, too. Thus,

Downloaded At: 12:45 15 January 2011

TABLE IIa

Transition temperatures $T_{1/2}$, activation energies E^a_{HL} and frequency factors A_{HL}, and k_{HL}(295 K) for some spin-crossover compounds in solution.

Compound Solvent	$T_{1/2}$ [K]	E^a_{HL} [cm^{-1}]	A_{HL} [s^{-1}]	k_{HL}(295 K) [s^{-1}]	Ref.
$[Fe(pybimH)_3](BPh_4)_2$ in MeOH/acetone/H_2O	232	850	1.4×10^8	2×10^7	[32a,c]
$[Fe(phenmethoxa)_2](BF_4)_2$ in acetone	250	930		1.4×10^6	[32b]
$[Fe(paptH)_2]Cl_2$ in H_2O	264	1497	1×10^{10}	7×10^6	[31]
$[Fe(pyimH)_3](BPh_4)_2$ in MeOH/acetone/H_2O	298	1135	2×10^9	1×10^7	[32a,c]
$[Fe(mepy)_2(py)tren](PF_6)_2$ in MeOH/acetone/H_2O	320			5×10^6	[30]
$[Fe(biz)_2](ClO_4)_2$ MeCN	~300			1.9×10^7	[25]
$[Fe(tpchxn)](ClO_4)_2$ in MeCN	321	350	8×10^8	1.4×10^7	[32c]
$[Fe(tppn)](ClO_4)_2$ in DMF	355	640	4×10^8	1.6×10^7	[32c]
$[Fe(HB(pz)_3)_2]$ in CH_2Cl_2/MeOH	369	420	2×10^8	2×10^7	[31]
$[Fe(ppa)_2](ClO_4)_2$ in acetone	387	1320	4×10^9	6×10^6	[25]
$Fe(tpmba)](ClO_4)_2$ in DMF	400	960	7×10^9	6.3×10^7	[32c]
$Fe(mepy)(py)_2tren](PF_6)_2$ in MeOH/acetone/H_2O	450			5×10^6	[30]
$[Fe(tptn)_3]^{2+}$ in H_2O	low-spin			6×10^8	[20]
$[Fe(bipy)_3]^{2+}$ in H_2O	low-spin			1.2×10^9	[26]
$[Fe(phen)_3]^{2+}$ in H_2O	low-spin			2×10^9	[33]

Downloaded At: 12:45 15 January 2011

as in solution, only spin-crossover compounds with $T_{1/2}$ around room temperature are suitable for such experiments (see Table IIb).

With the discovery of the light-induced spin transitions at low temperatures a systematic study of the LS ⇄ HS relaxation over a much larger temperature interval, namely 10 to 300 K, and for compounds with $T_{1/2}$ as low as 70 K all the way to low-spin systems with $T_{1/2}$ well in excess of 300 K became possible. It soon emerged that tunnelling processes are very important, becoming dominant at temperatures below ~100 K.[11,12] Figure 3 shows the HS → LS relaxation rate constants for a series of dilute single crystals plotted as $\ln[k_{HL}(T)]$ versus $1/T$. The deviation from Arrhenius behaviour is obvious. Table III gives the low temperature tunnelling rate constants $k_{HL}(T \to 0)$ and the activation parameters for this series of complexes.

TABLE IIb

Transition temperatures $T_{1/2}$, activation energies E^a_{HL} and frequency factors A_{HL}, and k_{HL}(295 K) from Mössbauer line-shape analysis for some spin-crossover compounds in the solid state.

	$T_{1/2}$ [K]	E^a_{HL} [cm^{-1}]	A_{HL} [s^{-1}]	k_{HL}(295 K) [s^{-1}]	Ref.
[Fe(pic)$_3$]Cl$_2$·MeOH	150	1050	2×10^9	7×10^6	[34b]
[Fe(pic)$_3$](PF$_6$)$_2$	185	1058	1.3×10^9	6.6×10^6	[34a]
[Fe(mtz)$_6$](PF$_6$)$_2$	205			2.5×10^6	[34d]
[Fe(mepy)$_3$tren](PF$_6$)$_2$	220	420	3×10^7	3×10^6	[34c]
[Fe(tpen)](ClO$_4$)$_2$	420			$\sim 10^8$	[36]

In addition, it contains $T_{1/2}$ and, for comparison, k_{HL} extrapolated to room temperature using Eq. (3). The latter once again fall within the range 10^6–10^8 s^{-1}. In contrast to the room temperature data, $k_{HL}(T \rightarrow 0)$ spans 12 orders of magnitude, and as shown in Fig. 4, there is a clear correlation between it and $T_{1/2}$.

3.2 Theoretical Considerations

Obviously, in order to arrive at a coherent understanding of the LS $\rightleftarrows$ HS relaxation dynamics it is essential to consider the full wealth of experimental data simultaneously. In particular, since there are no fundamental differences between solution and solid state (in both, the spin transition is basically a unimolecular process, albeit influenced by the surrounding medium), the two should not be discussed separately!

It is also obvious that a classical or semiclassical approach to the LS $\rightleftarrows$ HS relaxation is not adequate for its description. In the following, therefore, a brief outline of the quantum mechanical approach is given. Buhks *et al.*[8] describe the LS $\rightleftarrows$ HS relaxation in terms of a radiationless nonadiabatic multiphonon process occurring between two distinct zeroth-order spin states characterised by different nuclear configurations. For Fe(II) with $\Delta S = 2$, higher order spin-orbit coupling provides the mixing of the two states required for such a transition to take place. In the case of Fe(II) spin-crossover compounds it is mainly the metal–ligand bond length which is subject to large changes. Thus the obvious choice for the reaction coordinate is the totally symmetric normal coordinate. This leads to the so-

Downloaded At: 12:45 15 January 2011

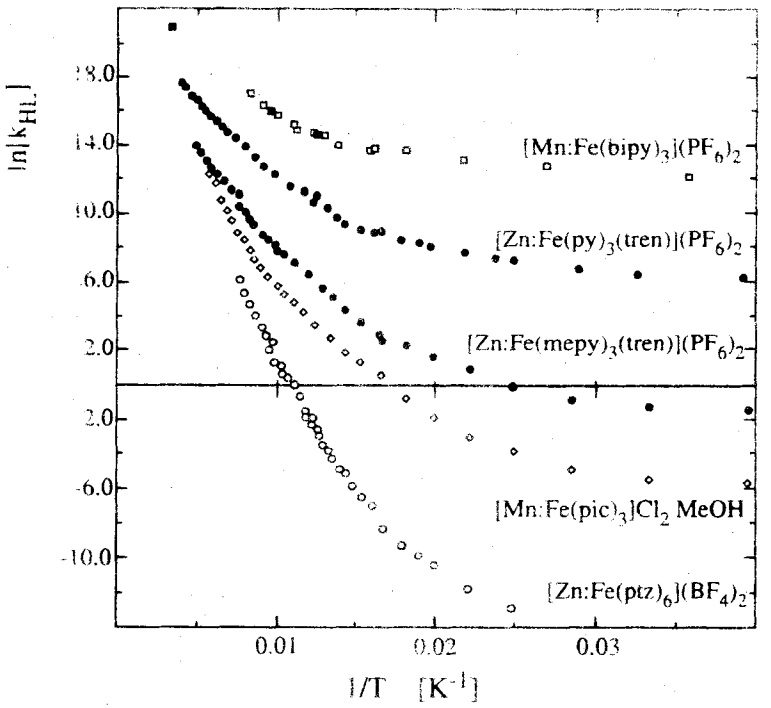

FIGURE 3 Experimental rate constants of the HS ⟶ LS relaxation plotted as ln[k_{HL}] versus $1/T$ (Arrhenius plot) for the dilute mixed crystal series (○) [Zn:Fe(ptz)$_6$](BF$_4$)$_2$, (◇) [Mn$_{1-x}$Fe$_x$(pic)$_3$]Cl$_2$·MeOH, (●) [Zn$_{1-x}$Fe$_x$(mepy)$_3$-tren](PF$_6$)$_2$, (●) [Zn$_{1-x}$Fe$_x$(py)$_3$tren](PF$_6$)$_2$, and (□) [Mn$_{1-x}$Fe$_x$(bipy)$_3$](PF$_6$)$_2$ using pulsed laser excitation. $x \approx 0.0005$ except for [Zn$_{1-x}$Fe$_x$(ptz)$_6$](BF$_4$)$_2$ for which $x \approx 0.1$. For comparison data for [Fe(bipy)$_3$]$^{2+}$ in solution (■) from Ref. 26 and for [Mn$_{1-x}$Fe$_x$(bipy)$_3$](PF$_6$)$_2$ from the Mössbauer emission study (□) of Ref. 28 are included.

called single configurational coordinate (SCC) model, where the potentials are taken to be displaced relative to each other by ΔQ_{HL} along a single normal coordinate Q only. Using Fermi's Golden Rule and the Condon approximation the rate constant for an intersystem crossing process can be expressed as[6]

$$k_{isc} = \frac{2\pi}{\hbar^2\omega}\,\beta_{isc}^2 g_f F_f(T). \qquad (5)$$

The electronic matrix element $\beta_{isc} = \langle \Phi_{LS} | H_{SO} | \Phi_{HS} \rangle$ can be estimated

Downloaded At: 12:45 15 January 2011

TABLE III

Transition temperatures $T_{1/2}$, activation energies E^a_{HL} and frequency factors A_{HL} for the high temperature region, and low temperature tunnelling rate constants $k_{HL}(T \rightarrow 0)$ for some Fe(II) coordination compounds in the solid state and embedded in polymer matrices. For comparison values of k_{HL} extrapolated to room temperature are included.

	$T_{1/2}$ [K]	E^a_{HL} [cm^{-1}]	A_{HL} [s^{-1}]	k_{HL} $(T \rightarrow 0)$ [s^{-1}]	k_{HL} (295 K) [s^{-1}]
$[Zn_{1-x}Fe_x(ptz)_6](BF_4)_2$	95	1100	5×10^7	5×10^{-7}	$\sim 5 \times 10^5$
$[Mn_{1-x}Fe_x(pic)_3]Cl_2 \cdot EtOH$	76			6×10^{-6}	
$[Zn_{1-x}Fe_x(pic)_3]Cl_2 \cdot EtOH$	95			2.5×10^{-5}	
$[Mn_{1-x}Fe_x(pic)_3]Cl_2 \cdot MeOH$	118	1120	2×10^8	2.5×10^{-3}	$\sim 4 \times 10^6$
$[Zn_{1-x}Fe_x(pic)_3]Cl_2 \cdot MeOH$	140			9×10^{-3}	
$[Zn_{1-x}Fe_x(mepy)_3tren](PF_6)_2$	210	837	5×10^8	1.4×10^{-1}	$\sim 8 \times 10^6$
$[Fe(mepy)_2(py)tren]^{2+}$ in PMMA	270			$\sim 5 \times 10^1$	
$[Fe(mepy)(py)_2tren]^{2+}$ in PMMA	370			$\sim 2 \times 10^2$	
$[Zn_{1-x}Fe_x(py)_3tren](PF_6)_2$	>400	640	1×10^9	4×10^2	$\sim 5 \times 10^7$
$[Mn_{1-x}Fe_x(bipy)_3](PF_6)_2$	low-spin			6×10^4	
$[Zn_{1-x}Fe_x(bipy)_3](PF_6)_2$	low-spin	364	2×10^9	6×10^5	$\sim 1 \times 10^9$
$[Fe(phen)_3]^{2+}$ in Nafion	low-spin			$\sim 5 \times 10^6$	

All values from Ref. 12a,b.

Downloaded At: 12:45 15 January 2011

to be ≈ 150 cm^{-1}, considering second order spin-orbit coupling via the low-lying $^3T_1$ state.[8] The electronic degeneracy of the final state g_f is equal to 1 for the HS $\rightarrow$ LS relaxation and equal to 15 for the LS $\rightarrow$ HS relaxation. For harmonic potentials with equal force constants f and equal vibrational frequencies $\hbar\omega$, the thermally averaged Franck–Condon factor $F_p(T)$ takes the form:

$$F_p(T) = \frac{\sum_m |\langle \chi_n | \chi_m \rangle|^2 \exp(-m\hbar\omega/k_BT)}{\sum_m \exp(-m\hbar\omega/k_BT)} . \qquad (6)$$

The reduced energy gap $p = \Delta E^0_{HL}/\hbar\omega$ is a measure for the vertical displacement of the potential wells of the initial and final state relative

Downloaded At: 12:45 15 January 2011

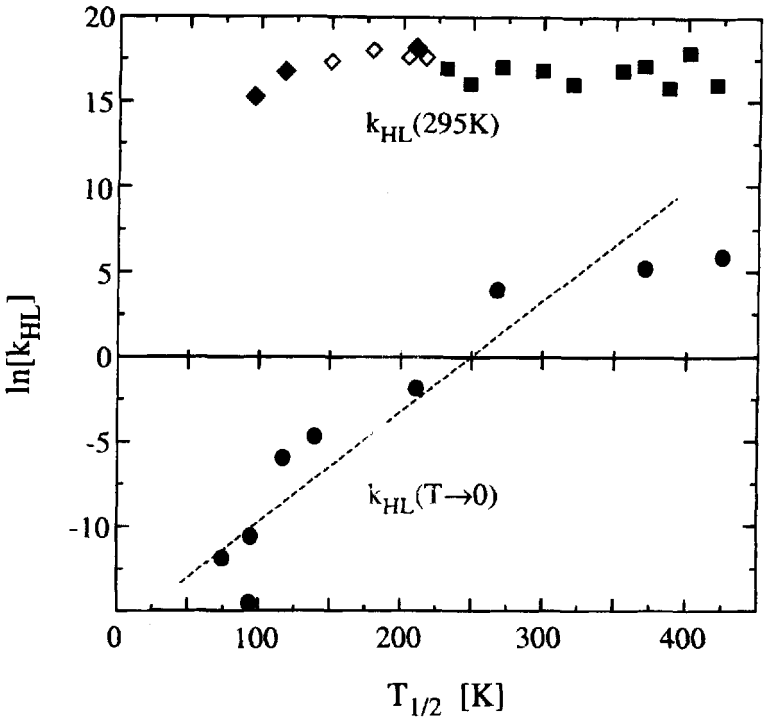

FIGURE 4 Experimental low-temperature tunnelling rate constants $k_{HL}(T \rightarrow 0)$ as a function of the transition temperature $T_{1/2}$ (●) from Table III, and k_{HL} at 295 K: experimental solution data (■), experimental solid state data from Mössbauer lineshape analysis (◇) and solid state data from pulsed laser excitation extrapolated to 295 K (◆).

to each other. The sum goes over all the vibrational levels m of the initial state, and the vibrational level of the final state $n = m + p$, in order to ensure energy conservation. For $T \rightarrow 0$, F_p simplifies to

$$F_p(T) = |\langle \chi_p | \chi_o \rangle|^2 = \frac{S^p e^{-S}}{p!}, \tag{7}$$

where the Huang–Rhys factor $S = (1/2) f \Delta Q_{HL}^2 / \hbar\omega$ is a measure for the relative horizontal displacement of the potential wells. For Fe(II)

compounds with an $[FeN_6]$ coordination, average values for f and $\hbar\omega$ are 2×10^5 dyn/cm and 250 cm^{-1}, respectively. With $\Delta Q_{HL} = \sqrt{6}\,\Delta r_{HL} \approx 0.5$ Å, a value for S of ≈45 has been estimated.[1]

Whereas S is not expected to vary to a large extent within the series of compounds all having $[FeN_6]$ coordination, the zero-point energy difference and thus p will vary all the way from $p < 1$ for spin-crossover compounds having transition temperatures below 100 K to $p > 10$ for true low-spin compounds. Figure 5 shows $\ln(k_{HL})$ as a function of both p and T, calculated according to Eq. (5) with $S = 45$ and $\hbar\omega = 250$ cm^{-1}. In the so-called strong-coupling limit with $S \gg p$, the characteristic features of $k_{HL}(T)$ are a temperature independent tunnelling rate below 50 K and a thermally activated process at elevated temperatures. The low temperature tunnelling rate $k_{HL}(T \to 0)$ is predicted to increase exponentially with increasing p

$$k_{HL}(T \to 0) \sim \exp(\alpha p), \tag{8}$$

with $\alpha \approx \ln(S)$ for $S \gg p$ and small values of p,[35] whereas [illegible] temperature a much smaller dependence of k_{HL} on p is exp[illegible]

The vital parameters governing the temperature depende[illegible] the low temperature tunnelling rate are S and p. Estimating [illegible] structural data is, in principle, straightforward, but p is so[illegible] more difficult to get at. As discussed in Section 2, Fig. [illegible] shows ΔE^0_{HL} as a function of $T_{1/2}$ for the $[Fe(pic)_3]^{2+}$ series. Of [illegible] dividing ΔE^0_{HL} by $\hbar\omega$ in turn gives p as a function of $T_{1/2}$.

Classically the activation energy E^a is given by the Marcus equation:

$$E^a_{clas} = \frac{\hbar\omega S}{4}\left(1 - \frac{p}{S}\right)^2. \tag{9}$$

which is temperature independent. With the typical values of S and $\hbar\omega$, the activation energy for small values of p becomes 250 [illegible] which is clearly much larger than the experimentally determined values. In the theory of nonadiabatic multiphonon relaxa[illegible] the activation energy defined as $-d[\ln(k_{HL})]/d(1/k_BT)$ is temperature dependent, starting from zero in the low temperature tunnelling region and approaching the classical value only at $T \to \infty$ [illegible]

Downloaded At: 12:45 15 January 2011

Downloaded At: 12:45 15 January 2011

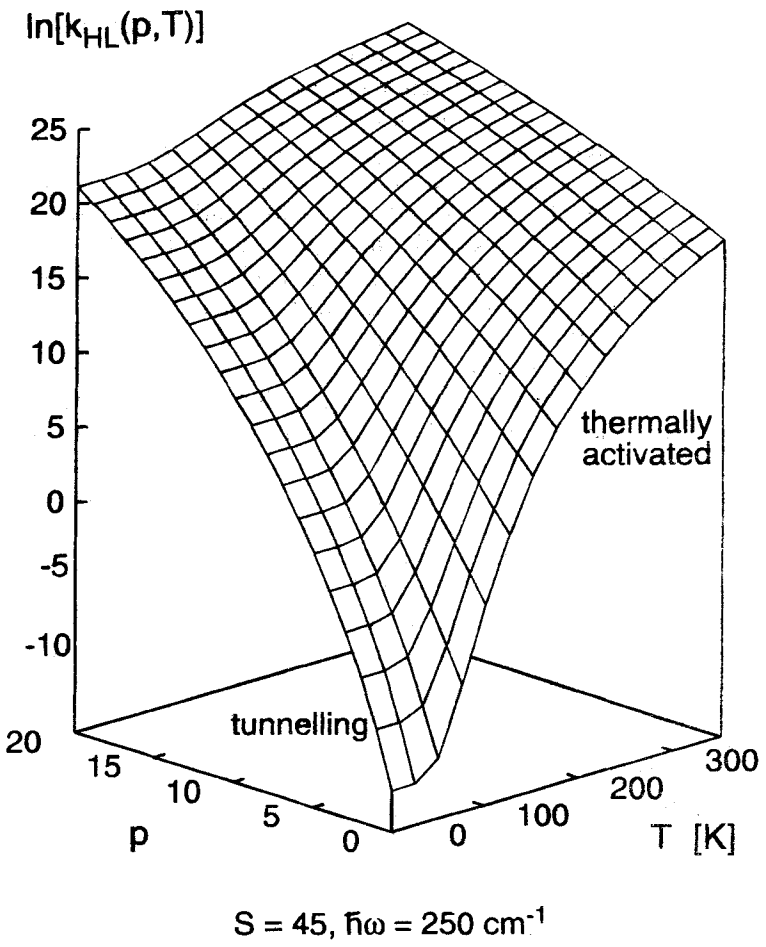

FIGURE 5 Parametric surface of $\ln[k_{HL}(p,T)]$ with a Huang–Rhys factor $S = 45$ and a vibrational frequency $\hbar\omega = 250\ cm^{-1}$ according to Eqs. (5) and (6).

6a shows the calculated temperature dependence explicitly for $S = 45$ and $\hbar\omega = 250\ cm^{-1}$, and different values of p. What does such a temperature dependent activation energy mean? According to Eq. (6) the thermally averaged Franck–Condon factor $F_p(T)$ is a sum over all vibrational levels m of products of Boltzmann factors $\exp(-m\hbar\omega/k_BT)$ times Franck–Condon factors $|\langle\chi_{m+p}|\chi_m\rangle|^2$. In Fig. 7a these two factors are plotted individually against m for several temperatures and $p = 1$. Clearly the overlap region is much below the classical crossing point of $m \approx S/4$. In Fig. 7b the product of the two as a function of m is shown, with T as parameter. The points to note are the following: (i) the integral under the curves, which is proportional to k_{HL}, increases with increasing temperature; (ii) the maximum goes to higher values of m with increasing temperature; (iii) the half-width is roughly four vibrational quanta. The first point is trivial, it just reflects the increase of k_{HL} with temperature. The second point is more interesting: the maximum gives the thermally populated vibrational level of the initial state from which the transition is most probable. It corresponds to the temperature dependent activation energy of Fig. 6. The width of the distribution shows that it is not just from the one level that the transition can occur. Although the maximum does shift towards the classical crossing point with increasing temperature, only a fraction of the molecules actually cross over classically even at room temperature.

Downloaded At: 12:45 15 January 2011

3.3 Discussion

The key features of the theory of nonadiabatic multiphonon relaxation in the strong vibronic coupling limit are the inverse energy gap law of Eq. (8) for $k_{HL}(T \to 0)$, and the activated region for $T > 100$ K. Qualitatively both are found experimentally. Quantitatively it is possible to go one step further. With the dependence of ΔE^0_{HL} on $T_{1/2}$ of Fig. 2 and the typical vibrational frequency $\hbar\omega = 250\ cm^{-1}$, the coefficient α in Eq. (8) can be estimated from Fig. 5 to be ≈ 4. This is in very good agreement with $\alpha \approx \ln(S)$ using $S \approx 45$, thus confirming the crucial estimate of S. With this value for α the more than 12 orders of magnitude increase of $k_{HL}(T \to 0)$ between the spin-crossover systems with $T_{1/2} < 100$ K and the low-spin systems with $T_{1/2} \gg 300$ K can be understood quantitatively. In fact, it is now possible to estimate p for the low-spin system $[Fe(bipy)]^{2+}$ with $k_{HL}(T \to 0) \approx 10^5$–$10^6\ s^{-1}$ to be ≈ 12, and therefore $\Delta E^0_{HL} \approx 3000\ cm^{-1}$.

Downloaded At: 12:45 15 January 2011

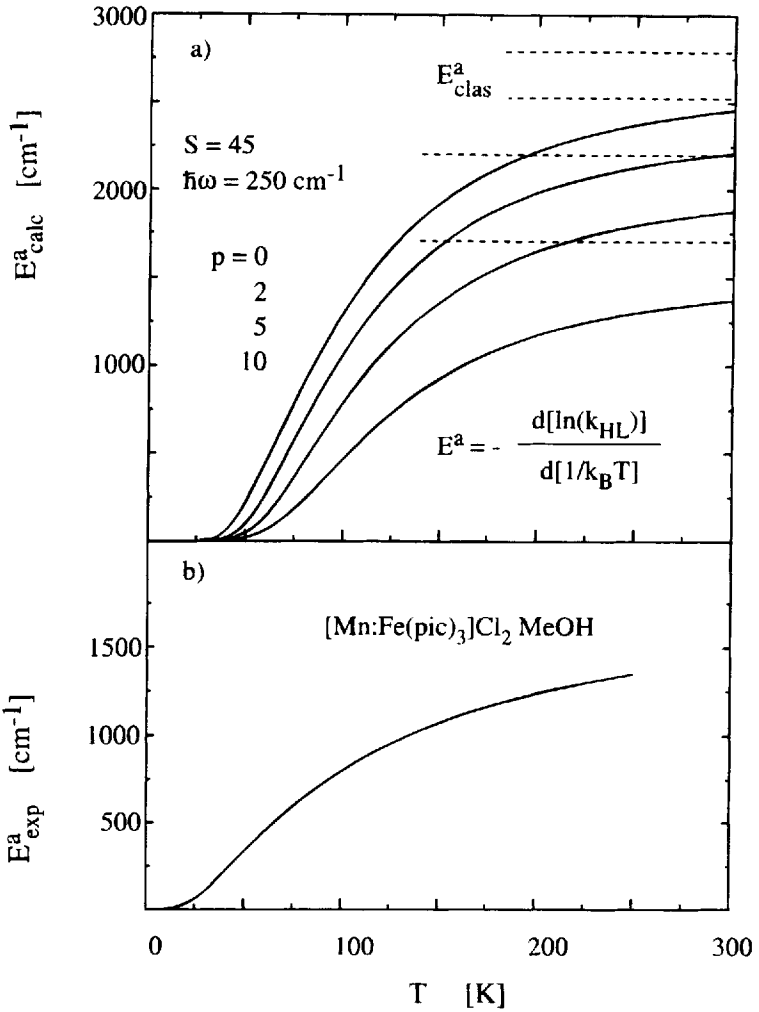

FIGURE 6 (a) Calculated temperature dependence of the activation energy predicted by the theory of nonadiabatic multiphonon relaxation in the strong vibronic coupling limit with $S = 45$ and $\hbar\omega = 250$ cm^{-1}. (b) Numerical evaluation of the effective activation energy from the experimental values of $k_{HL}(T)$ for $[Mn_{1-x}Fe_x(pic)_3]Cl_2 \cdot MeOH$ from Fig. 3.

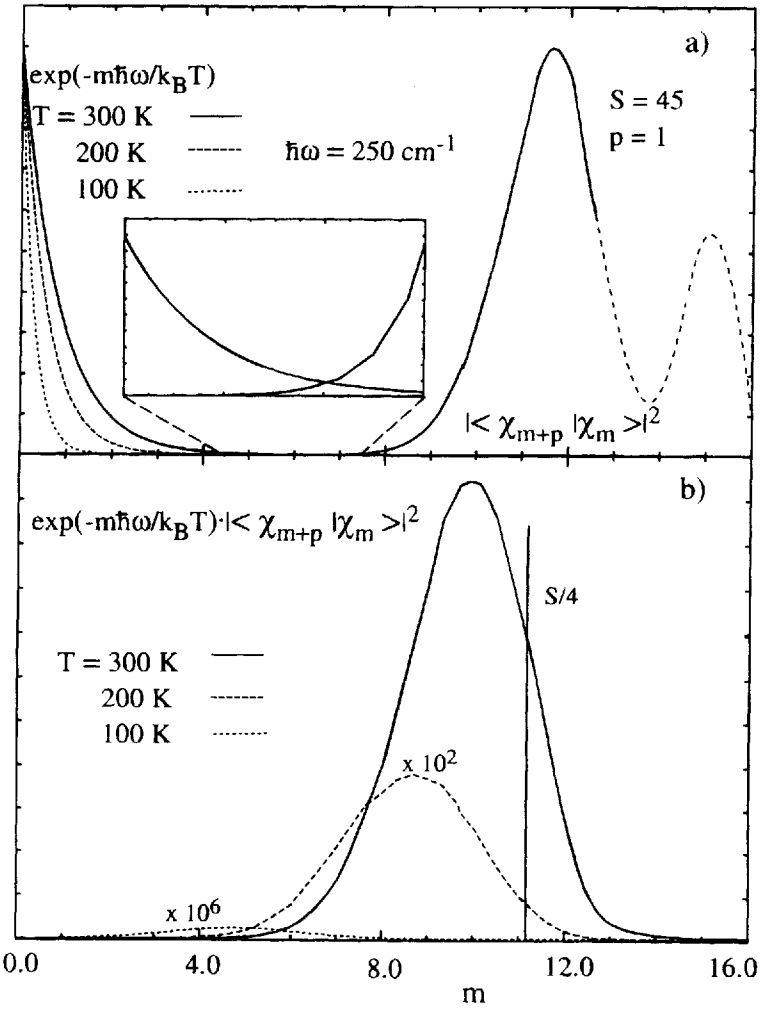

FIGURE 7 (a) The Boltzman factor $\exp(-m\hbar\omega/k_BT)$ for T = 100, 200 and 300 K and the Franck–Condon factor $|\langle\chi_{m+p}|\chi_m\rangle|^2$ as a function of the vibrational quantum number of the HS state m, calculated for S = 45, $\hbar\omega$ = 250 cm^{-1}, and p = 1. (b) Product of the Boltzman factor and the Franck–Condon factor as a function of m for T = 100, 200 and 300 K.

Downloaded At: 12:45 15 January 2011

The rate constants determined for spin-crossover complexes in solution and in the solid state extrapolated to room temperature fall within the comparatively small range 10^6–10^8 s^{-1}. Those of the low-spin systems are only one to two orders of magnitude larger. This much weaker dependence on p for the room temperature relaxation rates is as predicted. The experimental high temperature activation energies, although smaller than the classical values, should still track p and thus $T_{1/2}$ according to Eq. (9). Although showing a lot of scatter, they do indeed decrease with increasing $T_{1/2}$. For the solid state data, which generally has been determined over a much larger temperature interval, the tracking is better than for the solution data.

A further test is the dependence of the effective activation energy on temperature. Figure 6b shows this dependence determined numerically from the experimental values of $k_{HL}(T)$ for $[Mn_{1-x}Fe_x \cdot (pic)_3]Cl_2 \cdot UEtOH$. It follows the predicted increase from zero in the tunnelling region to an asymptotic value of $\sim$1500 cm^{-1} at high temperatures.

With hindsight, the rapidly interconverting complex [Fe(tpen)] $(ClO4)_2$ [36] behaves perfectly reasonably. It has a $T_{1/2}$ of 420 K and thus quite a large energy gap. The HS state only begins to be thermally populated above 320 K. According to Fig. 5, the rate constants for $p > 5$ and $T > 300$ K are expected to be $> 10^8$ s^{-1}. Thus, in the Mössbauer spectra a broadening of lines and even coalescence is expected in the temperature range where both species are present simultaneously.

Downloaded At: 12:45 15 January 2011

4. CONCLUSIONS

Because in spin-crossover systems there are no competing processes, HS $\rightarrow$ LS relaxation rate constants can be determined experimentally over a large temperature interval. This in turn allows a thorough test of the theory of radiationless multiphonon relaxation in the strong vibronic coupling limit. The basic message of this *Comment* is that ISC in Fe(II) spin-crossover complexes is a nonadiabatic process, that is, in a spontaneous transition electronic energy of the initial state is converted to vibrational energy in the final state. At low temperature the HS $\rightarrow$ LS relaxation is a pure tunnelling process, originating from the ground vibrational level of the HS state. The

12 order of magnitude increase of the low-temperature tunnelling rate from spin-crossover to low-spin compounds as well as the correlation with the zero-point energy difference can be understood quantitatively on the basis of the inverse energy gap law valid for $S \gg p$. Although at elevated temperatures quasi-classical behaviour is observed, the HS $\rightarrow$ LS relaxation still has to be considered a tunnelling process, but now originating from thermally populated vibrational levels of the HS state. It is therefore not appropriate to interpret experimentally determined activation energies within a classical framework and to identify them with saddle points of adiabatic potentials. The initial work on solution dynamics and Mössbauer lineshape analysis, being confined to a very small area on the parametric surface of Fig. 5, missed out on these essential points.

Of course, the picture developed here is still rather crude. The SCC model in its simplest form does not consider the more subtle characteristics of the various ligands. The values of the relevant parameters ($p, S, \hbar\omega, \beta_{HL}$) used in the calculations have to be regarded as typical values. In a more complete treatment these would have to be determined more accurately and for each complex individually. Thus the stiffness of, say, a cage complex[37] or the twisting motion in a tris-bidentate complex[32c] may influence the dynamics of the spin transition, and since most spin-crossover complexes possess rather low symmetry, there is in reality always more than one totally symmetric vibration to be considered.[17] Furthermore frequency shifts and anharmonicity would have to be considered, too. In contrast to the weak and intermediate coupling cases,[6,40] these only play a minor role in the strong coupling limit, even though with the large value of Δr_{HL} they are substantial. In this case this comes about because as the force constant on the one potential is increased from the mean value and the one on the other potential is decreased, the Franck–Condon factor stays approximately the same, and because the effects of anharmoncity cancel in a similar fashion.

The value for the electronic matrix element, too, would have to be calculated for each complex individually. However, in the Condon approximation there is not much latitude. Thus, in a severely distorted molecule, a somewhat larger value than the one used here might be more appropriate,[32c] but the much smaller values of 10 cm^{-1} and less,[10,30a] which have to be invoked for a classical interpretation of

Downloaded At: 12:45 15 January 2011

the room-temperature data using the Landau–Zener formalism, are highly unlikely.

What can be inferred from the above for other spin-crossover compounds or indeed for intersystem crossing processes in transition metal complexes in general? For the d^5 spin-crossover systems of Fe(III) with a $^2T_2 \rightleftarrows {}^6A_1$ spin transition, the bond length difference Δr_{HL} is only ~0.10–0.14 Å,[30] because compared to Fe(II) there is less d-π^* backbonding in the LS state. This results in a substantially smaller value for one of the vital parameters, namely the Huang–Rhys factor S. Using a typically 50% higher vibrational frequency than for the Fe(II) systems, a value for S of ~25 can be estimated for the Fe(III) systems. According to Eq. (7), the low-temperature tunnelling rate constants are therefore expected and indeed found to be seven to eight orders of magnitude larger for Fe(III) spin-crossover compounds than those for Fe(II) spin-crossover compounds, that is, $k_{HL}(T \rightarrow 0) \sim 10^2\ s^{-1}$ as compared to $10^{-5}\ s^{-1}$ for small values of p.[38] For the d^7 spin-crossover systems of Co(II) with the $\Delta S = 1$ spin equilibrium $^2E \rightleftarrows {}^4T_2$, Δr_{HL} is even smaller,[39] and therefore the relaxation rates are expected to be even larger. These differences of many orders of magnitude are only expected at low temperatures, at room temperature the relaxation in Fe(III) spin-crossover compounds is typically only one order of magnitude faster than in the Fe(II) compounds.[9] Thus, once again, to really track down the differences between the two, low-temperature data are essential.

All this has general implications for ISC in coordination compounds. It shows just how susceptible ISC rate constants are to small changes in structural and energetic parameters. Both have to be accurately known in order to calculate rate constants. In spin-crossover systems they can be determined independently, but in most systems, as for instance the Cr(III) compounds, where the interesting ISC processes occur between higher excited states, they can only be estimated indirectly. In addition, the determination of rate constants is very often only possible over a very limited temperature interval, because of competing processes. Thus, more often than not, clear-cut statements are not possible and, if they are attempted just the same, lead to controversies.

Downloaded At: 12:45 15 January 2011

APPENDIX: TABLE OF CHEMICAL ABBREVIATIONS

Rtz	1-alkyltetrazole (p = propyl-, m = methyl)
pic	2-picolylamine
$(mepy)_{3-x}(py)_x$tren	tris[(6-R)-2-pyridyl]-3-aza-6-butenyl]amine, R = H, CH_3
bipy	2,2′-bipyridine
phen	1,10-phenantroline
pybimH	2-(2′-pyridyl)benzimidazole
pyimH	2-(2′-pyridyl)imidazoel
phenmethoxa	3-[2-(1,10-phenantrolyl)-5-methyl-1,2,4-oxadiazole
paptH	2-(2-pyridylamino)-4-(2-pyridyl)thiazole
biz	2,2′-bi-1,4,5,6-tetrahydropyrimidine
$HB(pz)_3$	hydro-tris(pyrazoyl)borate
ppa	N2-(2-pyridylmethyl)picolylamidine
tppn	tetrakis(2-pyridylmethyl)-1-methyl-1,2-propanediamine
tptn	tetrakis(2-pyridylmethyl)-1,3-popylenediamine
tpmba	tetrakis(2-pyridylmethyl)-meso-2,3-butanediamine
tpchxn	tetrakis(2-pyridylmethyl)-1,2-cyclohexanediamine
tpen	tetrakis(2-pyridylmethyl)-1,2-ethylenediamine

Downloaded At: 12:45 15 January 2011

Acknowledgments

A considerable part of this work was performed while I was staying in the group of Prof. Philipp Gütlich in Mainz. I thank him for his kind hospitality and his encouragement. I also thank H. Spiering, P. Adler, A. Vef and R. Jakobi for most helpful discussions. This work was financially supported by the "Bundesministerium für Forschung und Technologie" (Germany), the "Deutsche Forschungsgemeinschaft" and the "Schweizerischer Nationalfonds".

References

1. T. H. Mayman, Nature **187**, 493 (1960).
2. M. Grätzel, Comments Inorg. Chem. **12**, 93 (1991).

3. J. F. Endicot, R. B. Lessard, D. Lynch, M. W. Perkovic and C. K. Ruy, Coord. Chem. Rev. **97**, 65 (1990) and references therein.
4. N. R. Kestner, J. Logan and J. Jortner, J. Phys. Chem. **78**, 2148 (1974).
5. R. Englman, *Nonradiative Decay of Ions and Molecules in Solids* (North Holland, Amsterdam, 1979).
6. C. J. Donnelly and G. F. Imbush, in NATO ASI **B245**, ed. B. DiBartolo (Plenum Press, New York, 1991), p. 175.
7. (a) R. B. Wilson and E. I. Solomon, J. Amer. Chem. Soc. **102**, 4085 (1980). (b) R. B. Wilson and E. I. Solomon, Inorg. Chem. **17**, 1729 (1978).
8. E. Buhks, G. Navon, M. Bixon and J. Jortner, J. Amer. Chem. Soc. **102**, 2918 (1980).
9. J. K. Beattie, Adv. Inorg. Chem. **32**, 1 (1988).
10. E. König, Structure and Bonding **76**, 51 (1991).
11. C.-L. Xie and D. N. Hendrickson, J. Amer. Chem. Soc. **109**, 6981 (1987).
12. (a) A. Hauser, A. Vef and P. Adler, J. Chem. Phys. **95**, 8710 (1991). (b) A. Hauser, Coord. Chem. Rev. **111**, 275 (1991).
13. (a) T. J. Meyer, Progress Inorg. Chem. **30**, 389 (1983). (b) N. Sutin, *ibid.*, p. 441.
14. (a) R. L. Martin and A. H. White, in *Transition Metal Chemistry*, Vol. **4**, ed. R. L. Carlin (Marcel Dekker, New York, 1986), p. 113. (b) H. A. Goodwin, Coord. Chem. Rev. **18**, 293 (1976). (c) P. Gütlich, Structure and Bonding **44**, 83 (1981). (d) H. Toftlund, Coord. Chem. Rev. **97**, 67 (1989).
15. (a) R. Jakobi, H. Spiering, L. Wiehl, E. Gmelin and P. Gütlich, Inorg. Chem. **27**, 1823 (1988). (b) R. Jakobi, H. Spiering and P. Gütlich, J. Chem. Phys. Solids **53**, 267 (1992).
16. P. Gütlich, A. Hauser and H. Spiering, to be published in Angew. Chemie.
17. A. Vef, U. Manthe, P. Gütlich and A. Hauser, submitted to J. Chem. Phys.
18. (a) S. Decurtins, P. Gütlich, C. P. Köhler, H. Spiering and A. Hauser, Chem. Phys. Lett. **139**, 1 (1984). (b) S. Decurtins, P. Gütlich, K. M. Hasselbach, H. Spiering and A. Hauser, Inorg. Chem. **24**, 2174 (1985).
19. A. Hauser, J. Chem. Phys. **94**, 2741 (1991).
20. (a) J. K. McCusker, K. N. Walda, R. C. Dunn, J. D. Simon, D. Magde and D. N. Hendrickson, J. Amer. Chem. Soc. **114**, 6919 (1992). (b) J. K. McCusker, K. N. Walda, R. C. Dunn, J. D. Simon, D. Magde and D. N. Hendrickson, J. Amer. Chem. Soc. **115**, 298 (1993).
21. M. A. Hoselton, L. J. Wilson and R. S. Drago, J. Amer. Chem. Soc. **97**, 1722 (1975).
22. (a) B. A. Katz and C. E. Strouse, J. Amer. Chem. Soc. **101**, 6214 (1979). (b) M. Mikami-Kido and Y. Saito, Acta Cryst **B38**, 452 (1982). (c) L. Wiehl, G. Kiel, C. P. Köhler, H. Spiering and P. Gütlich, Inorg. Chem. **25**, 1565 (1986). (d) L. Wiehl, H. Spiering, P. Gütlich and K. Knorr, J. Appl. Cryst. **23**, 151 (1990).
23. A. Hauser, Chem. Phys. Lett. **124**, 543 (1986).
24. (a) K.-U. Baldenius, A. K. Campen, H.-D. Hönk and A. J. Rest, J. Mol. Struct. **157**, 295 (1987). (b) A. Hauser, J. Adler and P. Gütlich, Chem. Phys. Lett. **152**, 468 (1988).
25. J. J. McGarvey and I. Lawthers, J. Chem. Soc. Chem. Commun. **1982**, 906.
26. A. D. Kirk, P. E. Hoggard, G. B. Porter and M. W. Windsor, Chem. Phys. Lett. **37**, 199 (1976).
27. A. Hauser, Chem. Phys. Lett. **173**, 507 (1990).
28. S. Deisenroth, A. Hauser, H. Spiering and P. Gütlich, to be published in Hyperfine Interactions.
29. I. Lawthers and J. J. McGarvey, J. Amer. Chem. Soc. **106**, 4280 (1984).

Downloaded At: 12:45 15 January 2011

30. (a) E. V. Dose, M. A. Hoselton, N. Sutin, M. F. Tweedle and L. J. Wilson, J. Amer. Chem. Soc. **100**, 1141 (1978). (b) M. A. Hoselton, R. S. Drago, L. J. Wilson and N. Sutin, J. Amer. Chem. Soc. **98**, 6967 (1976). (c) K. A. Reeder, E. V. Dose and L. J. Wilson, Inorg. Chem. **17**, 1071 (1978).
31. (a) J. K. Beattie, R. A. Binstead and R. J. West, J. Amer. Chem. Soc. **100**, 3044 (1978). (b) R. A. Binstead, J. K. Beattie, E. V. Dose, M. F. Tweedle and L. J. Wilson, J. Amer. Chem. Soc. **100**, 5609 (1978). (c) R. A. Binstead, J. K. Beattie, T. G. Dewey and D. H. Turner, J. Amer. Soc. **102**, 6442 (1980). (d) J. K. Beattie and K. J. McMahon, Austr. J. Chem. **41**, 1315 (1989).
32. (a) J. J. McGarvey, I. Lawthers, K. Heremans and H. Toftlund, J. Chem. Soc. Chem. Com. **1984**, 1575. (b) J. DiBenedetto, V. Arkle, H. A. Goodwin and P. C. Ford, Inorg. Chem. **24**, 456 (1985). (c) J. J. McGarvey, I. Lawthers, K. Heremans and H. Toftlund, Inorg. Chem. **29**, 252 (1990).
33. A. J. Street, D. M. Goodall and R. C. Greenhow, Chem. Phys. Lett. **56**, 326 (1978).
34. (a) P. Adler, H. Spiering and P. Gütlich, Inorg. Chem. **26**, 3840 (1987). (b) P. Adler, A. Hauser, A. Vef, H. Spiering and P. Gütlich, Hyp. Int. **47**, 343 (1989). (c) P. Adler, H. Spiering and P. Gütlich, J. Phys. Chem. Solids **50**, 587 (1989). (d) P. Adler, P. Poganiuch and H. Spiering, Hyp. Int. **52**, 47 (1989).
35. A. Hauser, Chem. Phys. Lett. **192**, 65 (1992).
36. H.-R. Chan, J. K. McCusker, H. Toftlund, S. R. Wilson, A. X. Trautwein, H. Winkler and D. N. Hendrickson, J. Amer. Chem. Soc. **112**, 6814 (1990).
37. L. L. Martin, R. J. Martin, A. Hauser, K. S. Hagen and A. M. Sargeson, J. Chem. Soc. Chem. Comm. **1988**, 1313.
38. S. Schenker and A. Hauser, J. Amer. Chem. Soc. **116**, 5497 (1994).
39. J. Zarembowitch, New J. Chem. **16**, 255 (1992).
40. C. W. Struck and W. H. Fonger, *Understanding Luminescence Spectra and Efficiencies Using Wp and Related Functions* (Springer-Verlag, Heidelberg, 1991).

Downloaded At: 12:45 15 January 2011